Silibinin Prevents TGFβ-Induced EMT of RPE in Proliferative Vitreoretinopathy by Inhibiting Stat3 and Smad3 Phosphorylation

Xinqi Ma,[1,2] Yiyu Xie,[1,2] Yajun Gong,[1,2] Chuxuan Hu,[1,2] Kairui Qiu,[1,2] Yao Yang,[1,2] Huangxuan Shen,[1,2] Xiaolai Zhou,[1,2] Chongde Long,[1,2] and Xiaofeng Lin[1,2]

[1]State Key Laboratory of Ophthalmology, Zhongshan Ophthalmic Center, Sun Yat-Sen University, Guangzhou, China
[2]Guangdong Provincial Key Laboratory of Ophthalmology and Visual Science, Sun Yat-Sen University, Guangzhou, China

Correspondence: Xiaolai Zhou, Zhongshan Ophthalmic Center, Sun Yat-sen University, 54 Xianlie Road, Guangzhou 510060, China; zhouxiaolai@gzzoc.com.
Chongde Long, Zhongshan Ophthalmic Center, Sun Yat-sen University, 54 Xianlie Road, Guangzhou 510060, China; longchd@mail.sysu.edu.cn.
Xiaofeng Lin, Zhongshan Ophthalmic Center, Sun Yat-sen University, 54 Xianlie Road, Guangzhou 510060, China; linxiaof@mail.sysu.edu.cn.

XM, YX and YG contributed equally to this work.

Received: July 2, 2023
Accepted: September 23, 2023
Published: October 31, 2023

Citation: Ma X, Xie Y, Gong Y, et al. Silibinin prevents TGFβ-induced EMT of RPE in proliferative vitreoretinopathy by inhibiting Stat3 and Smad3 phosphorylation. *Invest Ophthalmol Vis Sci.* 2023;64(13):47. https://doi.org/10.1167/iovs.64.13.47

Purpose. The purpose of this study was to investigate the effects of silibinin on epithelial-mesenchymal transition (EMT) of retinal pigment epithelial (RPE) and proliferative vitreoretinopathy (PVR) formation, as well as its underlying molecular mechanism.

Methods. Cellular morphological change and EMT molecular markers were evaluated by using phase contrast imaging, qPCR, and Western blot (WB) to investigate the impact of silibinin on the EMT of ARPE-19 cells. Scratch assay and transwell assay were used to study the effect of silibinin on cell migration. An intravitreally injected RPE-induced rat PVR model was used to assess the effect of silibinin on PVR in vivo. RNA-seq was applied to study the molecular mechanism of silibinin-mediated PVR prevention.

Results. Silibinin inhibited TGFβ1-induced EMT and migration of RPE in a dose-dependent manner in vitro. Moreover, silibinin prevented proliferative membrane formation in an intravitreal injected RPE-induced rat PVR model. In line with these findings, RNA-seq revealed a global suppression of TGFβ1-induced EMT and migration-related genes by silibinin in RPEs. Mechanistically, silibinin reduced TGFβ1-induced phosphorylation levels of Smad3 and Stat3, and Smad3 nuclear translocation in RPE.

Conclusions. Silibinin inhibits the EMT of RPE cells in vitro and prevents the formation of PVR membranes in vivo. Mechanistically, silibinin inhibits Smad3 phosphorylation and suppresses Smad3 nuclear translocation through the inhibition of Stat3 phosphorylation. These findings suggest that silibinin may serve as a potential treatment for PVR.

Keywords: proliferative vitreoretinopathy (PVR), epithelial-mesenchymal transformation (EMT), retinal pigment epithelial (RPE), silibinin

Proliferative vitreoretinopathy (PVR) is a blinding eye disease and the main cause of retinal detachment surgery failure. Five percent to 11% of patients with retinal detachment develop PVR.[1] Contraction of the proliferative membranes in PVR can lead to retinal detachment, which often results in significant vision loss.[2] Surgery is currently the most effective treatment for PVR but PVR often relapses. Despite advances in surgical techniques and instruments, the recurrent rate of PVR has remained largely unchanged.[3] Therefore, understanding the pathological mechanisms of PVR and searching for effective drugs that can prevent PVR formation is needed.

PVR formation is a fibrotic process, and the proliferative membrane within PVR contains multiple fibrous cellular components.[4] Among these fibrous cellular components, retinal pigment epithelial (RPE) is the most common cellular component in proliferative membranes.[5] Epithelial-mesenchymal transformation (EMT) of RPE cells is the core pathological process of PVR. EMT of RPE cells during PVR formation is characterized by the disruption of RPE cell polarity, the loss of intercellular tight junctions, the down-regulation of epithelial markers, and the upregulation of mesenchymal markers.[6] Following the initiation of EMT, RPE cells detach from Bruch's membrane and migrate into epi- and sub-retina spaces, and ultimately transform into αSMA-positive myofibroblast, the primary cell type responsible for the contraction of the proliferative membrane.[7,8] TGFβ, an effective cytokine to induce the EMT process, has been detected as one of the most abundant cytokines in the vitreous of patients with PVR.[9] Thus, TGFβ serves as the most important inducer of EMT during PVR formation.

Silibinin is a polyphenolic flavonoid extracted from milk thistle (Silybum marianum) and has been shown to have multiple biological properties, including antifibrosis, anti-inflammation, anti-oxidation, and anti-angiogenesis.[10] Due to its strong antifibrotic effect, silibinin has been already applied clinically to treat several fibrotic diseases, such as cirrhosis and chronic hepatitis.[11,12] Most recently, multiple

studies have demonstrated that silibinin can also inhibit the EMT of different types of tumor cells thereby suppressing tumor metastasis.[13–15] However, its role in the EMT of RPE cells during PVR formation remains to be explored. In this study, we investigated the effect of silibinin on the EMT model of RPE cells and a rat model of PVR. We found that silibinin inhibited TGFβ1-induced EMT and cell migration in vitro and attenuated the formation of PVR in vivo. Mechanistically, silibinin decreased TGFβ1-induced phosphorylation levels of Smad3 and Stat3, and Smad3 nuclear translocation in RPE. These findings suggest that silibinin may serve as a potential treatment for PVR.

Materials and Methods

Cell Culture and Reagent

Human RPE cells (ARPE-19; ATCC) were cultured in DMEM/F-12 (Gibco) supplemented with 10% fetal bovine serum (FBS; Gibco) and 1% 100 U/mL penicillin and 100 µg/mL streptomycin (Sigma-Aldrich) and maintained at 37°C in a 5% CO2 atmosphere. Silibinin (Sigma-Aldrich) was dissolved in dimethyl sulfoxide (DMSO). Then, 10 ng/mL TGFβ1 (Novoprotein) was used for inducing EMT of ARPE-19 cells, as described previously.[16]

Cell Apoptosis Assay

Apoptosis assay was performed as described previously,[17] using the Multicaspase Kit (Millipore Corporation, Hayward, CA, USA). The apoptosis rate of ARPE-19 cells was measured by the Muse Cell Analyzer (Millipore).

Scratch Assay

ARPE-19 cells were seeded in 35 mm dishes. Scratches were made by using 200 µL plastic pipette tips when the cell density reached 80%. After washing with PBS, the cells were treated with silibinin in the presence or absence of TGFβ1 for 72 hours. The scratches were observed and photographed using an optical microscope (Nikon) at 0 and 72 hours. The wound areas were measured by Image J software (National Institutes of Health [NIH]) and the wound closure rate was calculated through $(A_0 - A_{72})/A_0$* 100% (A_0 is the wound area at 0 hours, and A_{72} is the wound area at 72 hours).

Transwell Assay

The 24-well plates with polycarbonate membranes (Corning) were applied for transwell assay. ARPE-19 cells at the density of 4*10^4 were suspended in 200 µl serum-free medium and seeded in the upper chambers. Then, 500 µL of medium containing 20% FBS were added into the lower chambers. ARPE-19 cells in the upper chambers were treated with silibinin in the presence or absence of TGFβ1 for 48 hours. Then, the migrated cells were fixed with 4% paraformaldehyde and stained with crystal violet (Solarbio) at room temperature for 15 minutes. The migrated cells were captured at 48 hours. The numbers of migrated cells were counted by Image J software (NIH).

Quantitative Real-Time PCR

Total RNA of ARPE-19 cells was isolated using TRIzol reagent (Invitrogen) following the manufacturer's procedure. Then, 1 µg total RNA of ARPE-19 cells was transcribed using the PrimeScript II 1st Strand cDNA Synthesis Kit (TaKaRa). Quantitative real-time PCR (qRT-PCR) was conducted using the LightCycler 96 (Roche) with the SYBR Premix Ex TaqTM Kit (TaKaRa). The sequences of primers are presented in Supplementary Table S1.

Western Blot

Total proteins from ARPE-19 cells were extracted with NP40 supplemented with proteinase inhibitors, phosphatase inhibitors, and PMSF (Sigma-Aldrich). The cytoplasmic and nuclear-enriched proteins were isolated following the administration of BBproExtra plasmic and nuclear protein isolation kit (BB-31122, Bestbio). Protein concentration was measured using the BCA assay (Thermo Fisher Scientific). The protein samples were separated by 8% or 10% SDS-PAGE gels and transferred to PVDF membranes (Millipore). The membranes were blocked with 5% non-fat milk and then incubated with primary antibody at 4°C overnight. The next day, the membranes were incubated with HRP-conjugated secondary antibodies (Abcam) and proteins were detected by chemiluminescence. Primary antibodies included: MMP2 (1:1000, 40994; CST), COL1A1 (1:1000, #81375; CST), Fibronectin (1:1000, #26836; CST), N-cadherin (1:10000, #70611; Abcam), phospho-SMAD3 (Ser423/425, 1:1000, #9520; CST), SMAD3 (1:1000, #9523; CST), phospho-STAT3 (Y705, 1:1,000, ab267373; Abcam), STAT3 (1:1000, #4904; CST), GAPDH (1:10000, #5174; CST), β-actin (1:10000, #4970; CST), and Histone-H3 (1:5000, ab1791; Abcam). Bands of Western blot were quantified using Image J (NIH).

Establishment of the PVR Rat Model

All animal procedures were carried out following the guidelines of the Animal Care and Use Committee of Sun Yat-sen University, and handled according to the ARVO Statement for the Use of Animals in Ophthalmic and Vision Research. Long Evans rats (aged 6–8 weeks, weight = 200 ± 10 g) were purchased from the Charles River (Weitong Lihua Co. Ltd.). The rats were anesthetized and their pupils were dilated before vitreous injection. To induce PVR, suspension of ARPE-19 cells (3 µL, 1 × 10^5 cells per µL) with 10 ng/mL TGFβ1 were injected into the vitreous of long-Evans rats with a 33G Hamilton syringe, and the injected eyes were treated with antibiotic eye drops and ointment after the operation. The PVR stages of all injected eyes were determined by two masked observers at 7, 14, and 21 days after injection, following the rat PVR grading scale[18]: stage 0 = no proliferative response; stage 1 = intravitreal proliferation; stage 2 = epiretinal membrane formation with retinal folds; and stage 3 = white dense membrane covering the retina, with retinal folds and localized retinal detachments with or without a localized posterior capsular cataract. The rat fundus images were captured using the retinal imaging system (Phoenix Micron IV).

Hematoxylin and Eosin Staining

The rat eyeballs were fixed in 10% neutral buffered formalin (NBF; Thermo Fisher Scientific) and then embedded in paraffin and sliced into 5 µm thickness. After immersion in xylene and ethanol (100%, 90%, 80%, and 70%) for deparaffinization and rehydration, the slides were then immersed in tap water. Slices were stained with hematoxylin for 8 minutes

Investigative Ophthalmology & Visual Science

and rinsed with tap water, subsequently differentiated in hydrochloric ethanol for 60 seconds. Then the slides were stained with eosin for 60 seconds and then dehydrated quickly in ethanol (70%, 80%, 90%, and 100%) and cleared in xylene. The eyeball slides were mounted with polystyrene mountant, and images were captured with a light microscope.

Immunofluorescence

The coverslips with ARPE-19 cells or deparaffined rat eyeball sections were fixed with 4% paraformaldehyde for 15 minutes, and blocked in goat serum with 0.3% Triton for 60 minutes at room temperature. Subsequently, the cells or eyeball tissues were incubated with primary antibody at 4°C overnight. The next day, the cells or eyeball tissues were incubated with secondary antibodies (anti-rabbit Alexa 488 and anti-mouse Alexa 594; Thermo Fisher Scientific), followed by DAPI staining. The immunofluorescence was detected by a confocal laser scanning microscope (Zeiss). Primary antibodies included: FN (1:500, #26836; CST), αSMA (1:500, #419245; CST), and SMAD3 (1:500, #9523; CST).

RNA-Sequencing

The total RNA of ARPE-19 cells was isolated using TRIzol reagent (Invitrogen) following the manufacturer's procedure. After measuring RNA integrity number (RIN) with a Bioanalyzer 2100 (Agilent) and confirmed by electrophoresis with denaturing agarose gel, the cDNA library (300 $\pm$ 50 bp) was established. Subsequently, the 2 $\times$ 150 bp paired-end sequencing (PE150) on an Illumina Novaseq 6000 was performed. The StringTie software was used to quantify transcripts by calculating FPKM, and the edgeR package was used to analyze differentially expressed genes (DEGs) between samples. The mRNAs with a fold change >2 and a $P < 0.05$ were defined as DEGs with statistical significance. Finally, the DAVID software was used to perform Gene Ontology (GO) and Kyoto Encyclopedia of Genes and Genomes (KEGG) enrichment analysis on the mRNAs.

Statistical Analysis

IBM SPSS version 21.0 and GraphPad Prism (version 9.0) were used for statistical analysis. Comparisons of PVR stages between the two groups were carried out by the Mann-Whitney U test. Multiple comparisons were carried out by One-way ANOVA followed by Dunnett's post hoc test. Data were presented as mean $\pm$ standard deviation (SD) of at least three independent experiments unless otherwise specified. Any $P < 0.05$ was defined as statistically significant.

Results

Silibinin Inhibits TGFβ1-Induced EMT of ARPE-19 Cells

To find suitable concentrations of silibinin for the EMT study, we first investigated the effect of silibinin on RPE cell apoptosis. As the flow cytometry results showed that the apoptosis of ARPE-19 cells significantly increased starting from the concentration of 400 µM (Supplementary Figs. S1A, S1B). Therefore, we chose the lower concentrations of silibinin (0, 50, 100, 150, and 200 µM) for subsequent experiments. To induce the EMT of RPE cells, we treated ARPE-19 cells with TGFβ1 for 48 hours. The phase-contrast images showed ARPE-19 cells underwent a morphological change from polygonal to elongated spindle-shaped ones, indicating effective induction of RPE cell EMT upon TGFβ1 treatment. This morphological change was inhibited by the treatment of silibinin (Fig. 1A). In line with these findings, qRT-PCR and Western blot results revealed a strong inhibition of silibinin on the expression TGFβ1-induced EMT genes, including COL1A1, MMP2, Fibronectin1, and N-cadherin (Figs. 1B–I).

To further investigate the effect of silibinin on TGFβ1-induced EMT of RPE cells, we performed bulk RNA sequencing (RNA-seq; Fig. 2A). The volcano plot of the DEG analysis showed that, compared to the control group, 2024 genes were upregulated, and 712 genes were downregulated in the TGFβ1 treatment group (Fig. 2B). The GO analysis of the DEGs revealed that these changed genes are mainly involved in extracellular matrix organization, cytoskeleton remodeling, and mitosis (Supplementary Figs. S2A, S2B). As expected, gene set enrichment analysis (GSEA) revealed that TGFβ1 promotes the expression of EMT-related genes ($P < 0.05$; Supplementary Fig. S2C). In line with these findings, the cluster analysis demonstrated a global upregulation of EMT-related genes (Supplementary Fig. S2D). Compared with TGFβ1 alone, cotreatment of silibinin at 100 µM and 150 µM have a total of 7829 DEGs (5057 upregulated, and 2772 downregulated) and 11,798 DEGs (5430 upregulated, and 6368 downregulated), respectively (Figs. 2C, 2D). The GO analysis revealed these DEGs were also involved in extracellular matrix organization and cytoskeleton remodeling, suggesting the regulation of TGFβ1-induced genes by silibinin (Figs. 2E, 2F). In agreement with these findings, silibinin treatment significantly downregulated the EMT signaling pathway ($P < 0.001$; Fig. 2G) and EMT-related genes (Fig. 2H).

Silibinin Reduces ARPE-19 Cells Migration

Both epi-retinal and sub-retinal proliferative membrane formation require RPE cell migration from Bruch's membrane. To investigate the effects of silibinin on ARPE-19 cell migration, we performed the scratch assay and the transwell assay. As it showed, a 72-hour silibinin treatment significantly reduced the healing area of scratch in the presence (Figs. 3A, 3B) or absence (Supplementary Figs. 3A, 3B) of TGFβ1 in a dose-dependent manner. Consistent with scratch assay results, silibinin significantly reduced ARPE-19 cell migration either in the existence of TGFβ1 or not (Figs. 3C, 3D). In support of these findings, the bulk RNA-seq results revealed silibinin treatment significantly downregulated migration-related genes (Figs. 3E, 3F).

Silibinin Inhibits the Formation of Proliferative Membranes In Vivo

To investigate the role of silibinin on PVR formation in vivo, we used an intravitreal injected RPE-induced rat PVR model. Prior to and after ARPE-19 cells intravitreal injection, fundus images were taken to evaluate PVR formation. As the representative images showed TGFβ1-treated group started to form epi-retinal membranes (Fig. 4A, arrows) around the post-injection day (PID) 7 and developed retinal detachment around PID 14 (see Fig. 4A, asterisk). Silibinin treatment significantly reduced clinical score or PVR stages at PID 7 ($P < 0.05$), 14 ($P < 0.001$), and 21 ($P < 0.05$;

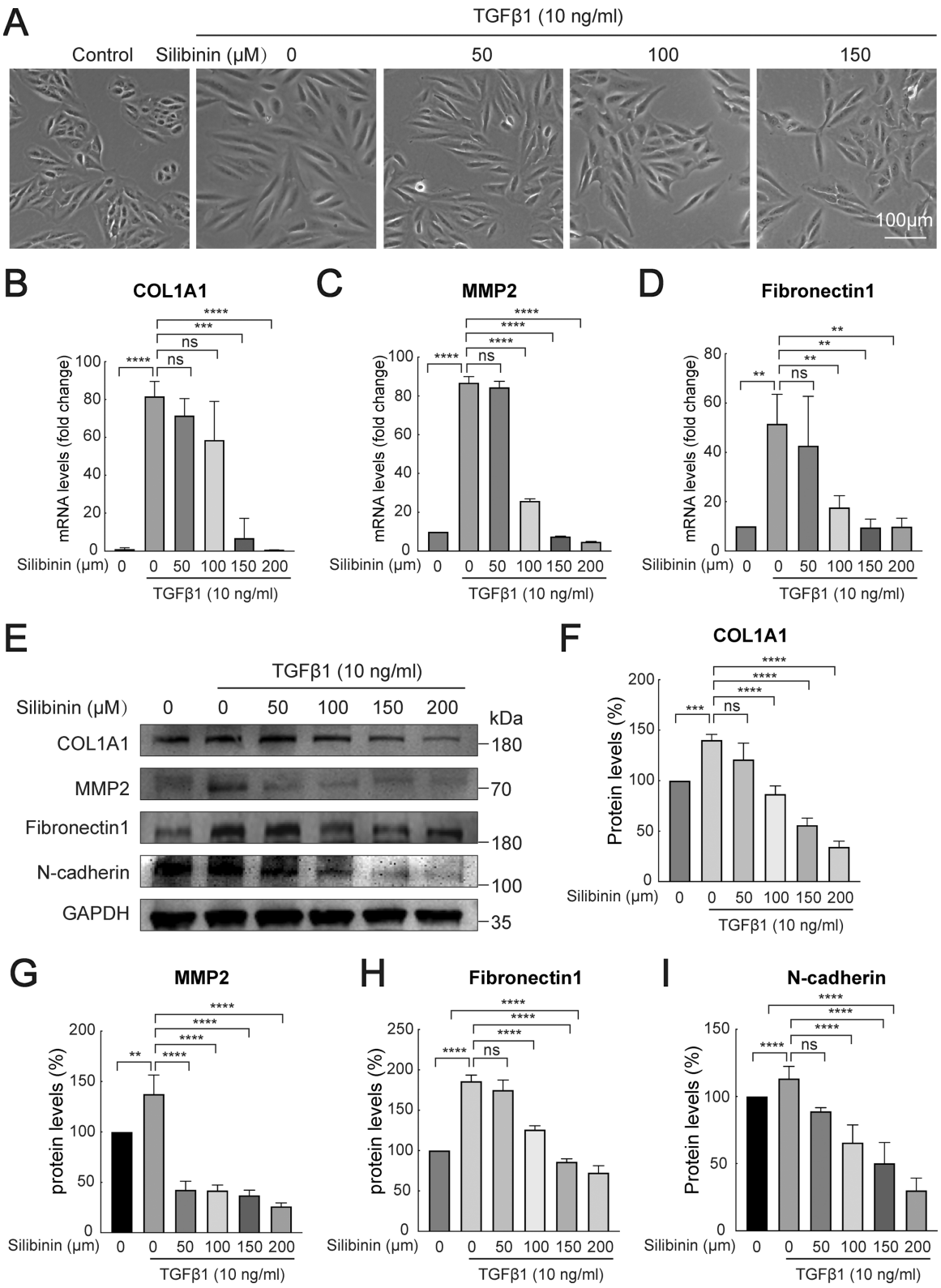

Figure 1. Effects of silibinin on EMT of ARPE-19 cells. (**A**) Representative images of the cell morphology change after the treatment with TGFβ1 alone and the combination with silibinin for 48 hours. (**B, C, D**) Real-time qPCR analysis of mRNA expression of COL1A1, MMP2, and Fibroectin1 after treatment with TGFβ1 alone and the combination with silibinin for 48 hours. (**E**) Western blot analysis of COL1A1, MMP2, Fibroectin1, and N-cadherin in ARPE-19, after treatment with TGFβ1 alone and the combination with silibinin for 48 hours. (**F, G, H, I**) Statistical analysis of the protein expression (data represent mean ± SD, $n = 3$, $^{**}P < 0.01$, $^{***}P < 0.001$, $^{****}P < 0.0001$).

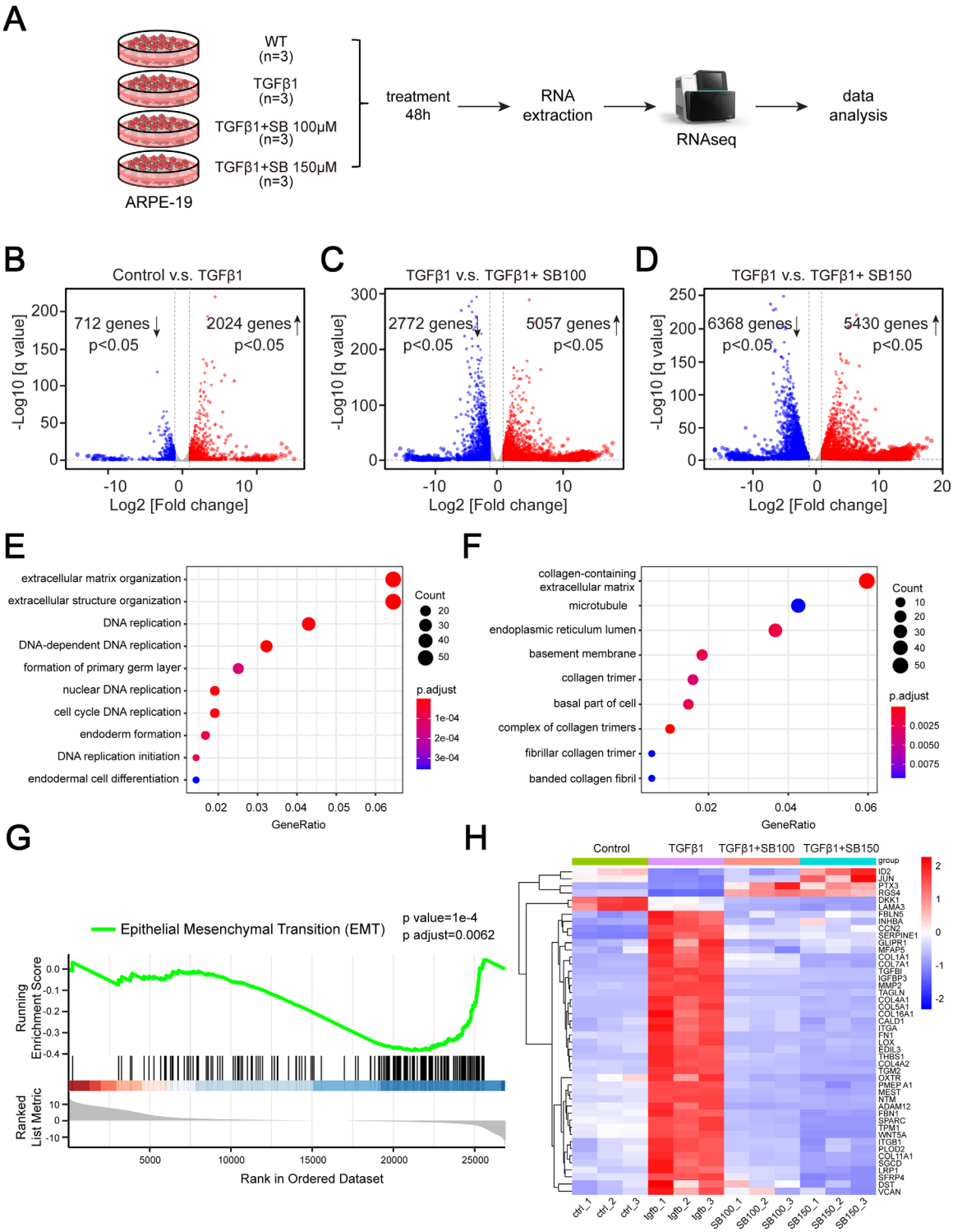

Figure 2. Bulk RNA-seq analysis of the effect of silibinin on TGFβ-induced EMT in ARPE-19 cells. (**A**) A schematic draw of the experimental design. (**B, C, D**) Volcano plots show DEGs between different treatments: TGFβ1 and control (**B**), TGFβ1 + silibinin 100 μM (TGFβ1 + SB100) (**C**), TGFβ1 + silibinin 150 μM (TGFβ1 + SB150) (**D**). (**E, F**) Gene Ontology (GO) analysis on the DEGs between TGFβ1 + silibinin (100 μM) and TGFβ1 alone: top 10 biological processes (**E**) and top 9 cellular components (**F**); (**G**) Gene set enrichment analysis (GSEA) shows a global suppression of EMT-related genes upon silibinin (100 μM) treatment, $P = 0.0001$. (**H**) Heatmap shows the top EMT-related DEGs that up- or downregulated by silibinin (100 μM) treatment (fold change ≥ 2, $P < 0.05$).

see Figs. 4A–D). These findings were further confirmed by pathological analysis. Representative hematoxylin and eosin (H&E) staining showed the formation of the epiretinal dense membrane with numerous cellular components (asterisk), swollen and shrunken retina tissue, and the detachment of the retina in the TGFβ1-treated group at PID 21 (Fig. 4E), whereas, the silibinin-treated group only showed mild shrinkage and swelling of retinas (see Fig. 4E).

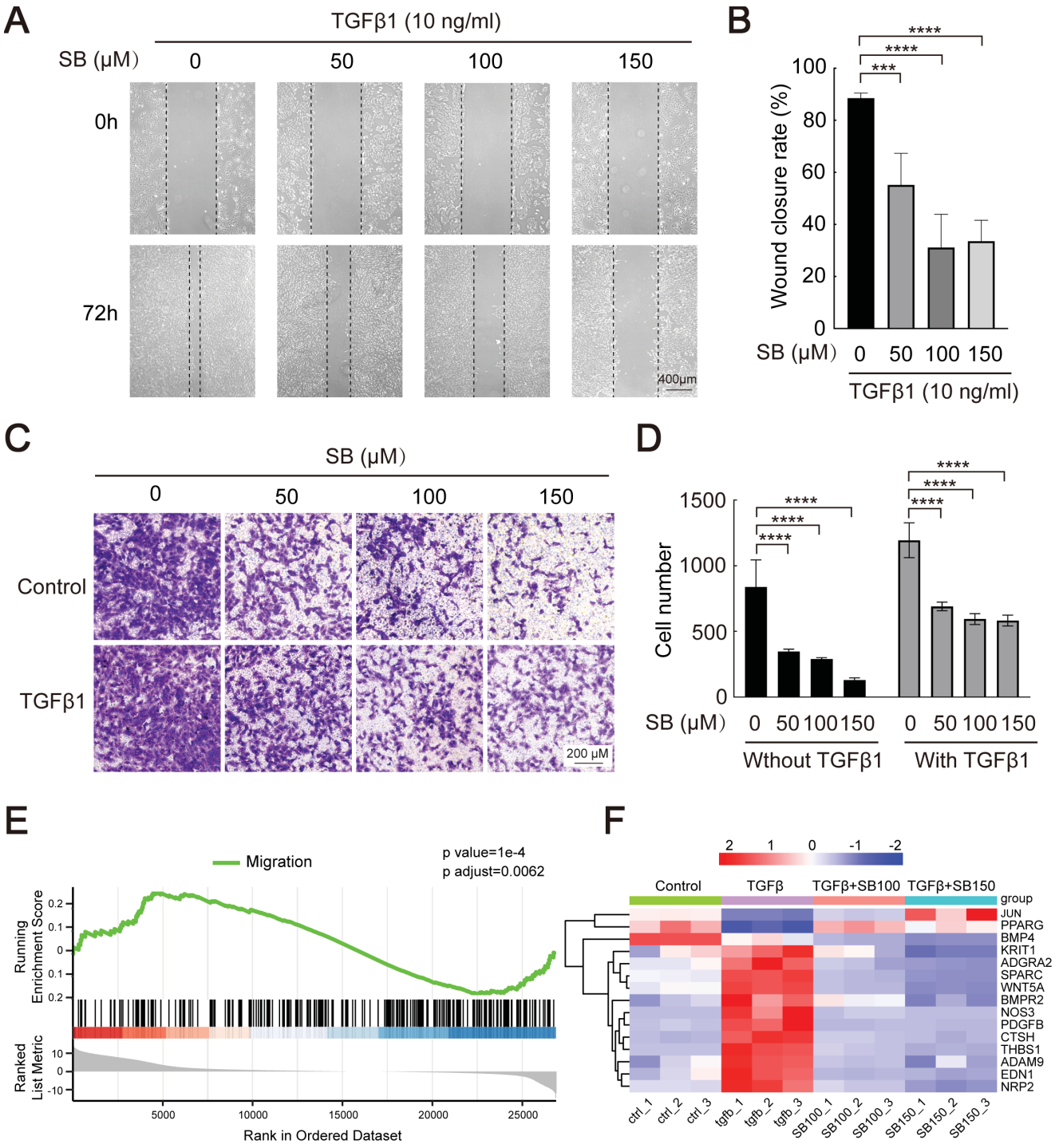

Figure 3. Effects of silibinin on ARPE-19 cell migration. (**A**) Representative images of scratch assay show the migration of ARPE-19 cells upon the treatment of the indicated concentrations of silibinin (SB) for 0 hours and 72 hours. (**B**) Quantification of the wound closure rate (%) by the measurement of the healing area of the scratch in **A**. The graph represents the mean ± SD ($n = 3$). Data were analyzed by One-way ANOVA followed by Dunnett's post hoc test. ***, $P < 0.001$, ****, $P < 0.0001$. (**C**) Representative images of the transwell assay show the migration of ARPE-19 cells upon the treatment of silibinin for 48 hours. (**D**) Quantification of the number of cells migrating through the transwell membrane. The graph represents the mean ± SD ($n = 5$). Data were analyzed by One-way ANOVA followed by Dunnett's post hoc test. ***, $P < 0.001$, ****, $P < 0.0001$. (**E**) Gene set enrichment analysis (GSEA) shows a global suppression of cell migration-related genes upon silibinin (100 μM) treatment, adjust $P = 0.0062$. (**F**) Heatmap shows the top cell migration-related DEGs that were up- or downregulated by silibinin (100 μM) treatment (fold change ≥ 2, $P < 0.05$).

Investigative Ophthalmology & Visual Science

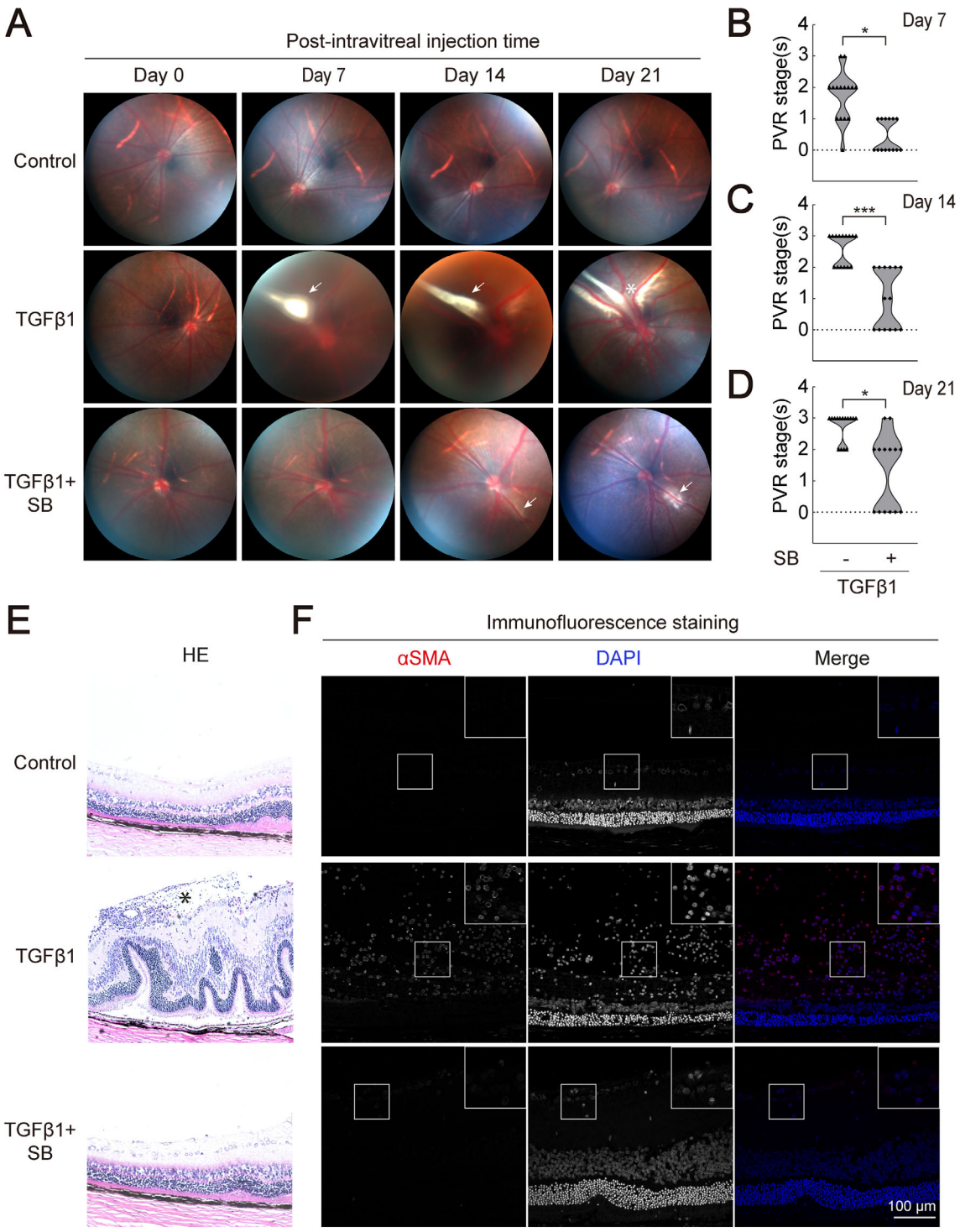

Figure 4. Effects of silibinin on PVR formation in vivo. (**A**) ARPE-19 cells were injected intravitreally to induce PVR formation in rats. Representative images of the rat fundus prior to and after intravitreal injection with PBS (control group), TGFβ1 + ARPE-19 cells (PVR model group), and TGFβ1 + ARPE-19 cells + silibinin (SB) (silibinin treated group), respectively. The *white arrow* indicates pre-retinal proliferation, and the *white asterisk* represents retinal detachment. (**B, C, D**) Statistical analysis of rat PVR stages distribution at day 7 (**B**), day 14 (**C**), and day 21 (**D**) after intravitreal injection. The graph exhibits the PVR grade of each rat. Data were analyzed by the Mann-Whitney *U* test ($n = 15$ in the PVR model group and $n = 14$ in the silibinin treated group). *$P < 0.05$, ****$P < 0.0001$. (**E**) Representative images of H&E staining of eyeballs collected from indicated groups at day 21 after intravitreal injection. The *black asterisk* indicates an epi-retinal dense membrane with numerous cellular components. (**F**) Representative images of αSMA (*red*) immunofluorescence staining of rat eyeballs collected from indicated groups at day 21 after intravitreal injection. Cell nuclei were stained with DAPI (*blue*).

Investigative Ophthalmology & Visual Science

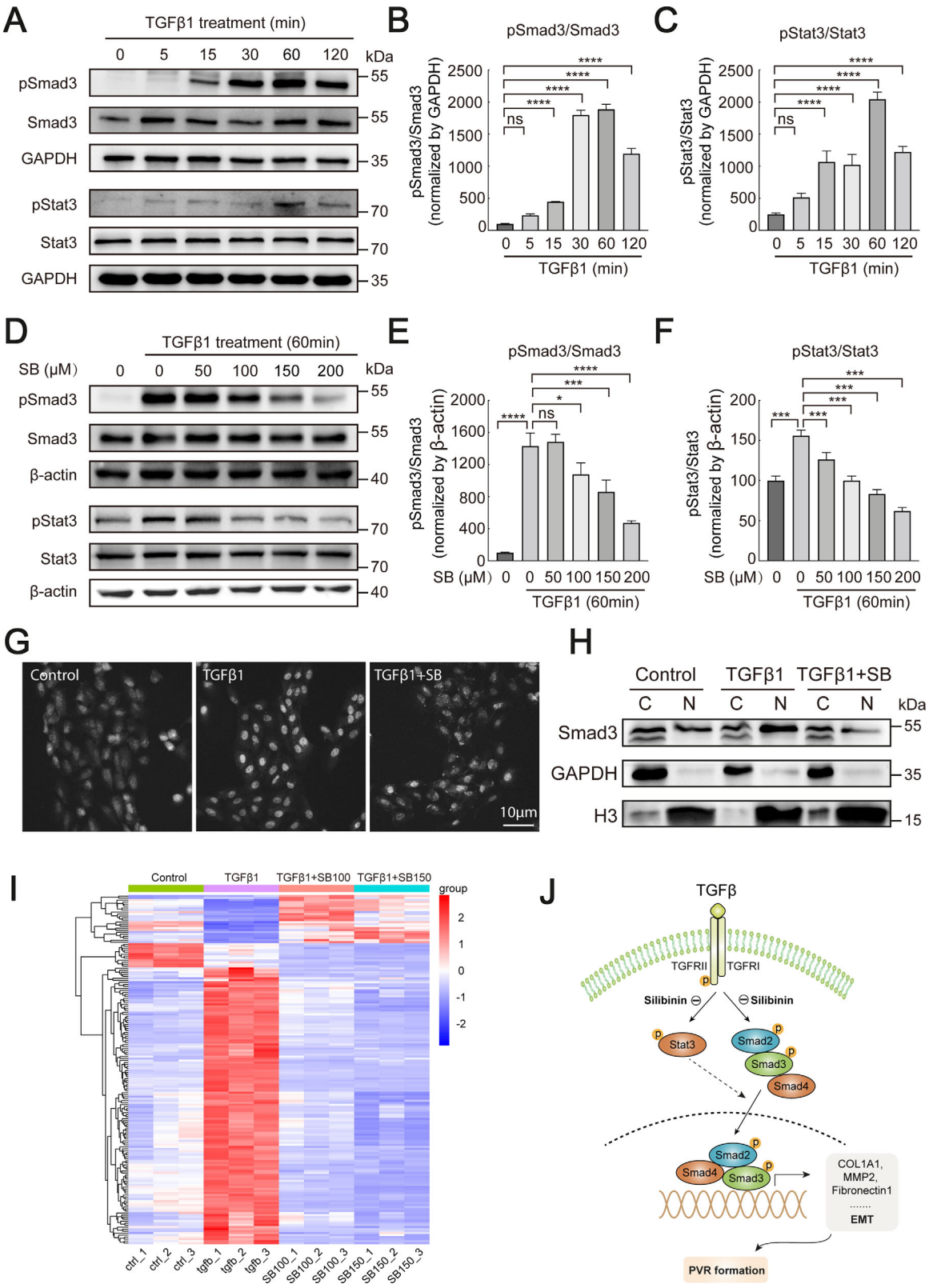

Figure 5. Effects of silibinin on Smad3 and Stat3 phosphorylation and Smad3 nuclear translocation. (**A**) Western blots show protein levels of pSmad3, Smad3, pStat3, and Stat3 after treatment with TGFβ1 for 0, 5, 15, 30, 60, and 120 minutes in ARPE-19 cells. (**B, C**) Quantification of the blots in **A**. Graphs represent the mean ± SD ($n = 3$). Data were analyzed by One-way ANOVA followed by Dunnett's post hoc test. ns = not significant, ****$P < 0.0001$. (**D**) Western blots show protein levels of pSmad3, Smad3, pStat3, and Stat3 after treatment with TGFβ1 and silibinin for 60 minutes in ARPE-19 cells. (**E, F**) Quantification of the blots in **D**. Graphs represents the mean ± SD ($n = 3$). Data were analyzed by One-way ANOVA followed by Dunnett's post hoc test. ns = not significant, *$P < 0.05$, ***$P < 0.001$, ****$P < 0.0001$. (**G**) Representative images of Smad3 immunofluorescence staining of control, TGFβ1-treated alone, and TGFβ1-silibinin (100

μM) co-treated ARPE-19 cells for 2 hours. (**H**) Representative Western blots from three independent experiments show protein levels of Smad3, histone H3, and GAPDH in the cell nucleus and cytoplasm of control, TGFβ1-treated alone, and TGFβ1 and silibinin (100 μM) co-treated ARPE-19 cells. (**I**) Heatmap shows the top cell TGFβ/Smad-dependent pathway-related DEGs that up- or downregulated by silibinin (100 μM) treatment (fold change ≥ 2, $P < 0.05$). (**J**) A diagram that shows the mechanism of Silibinin-mediated inhibition of TGFβ1-induced EMT of RPE in PVR.

Moreover, the immunofluorescence staining showed abundant αSMA positive myofibroblasts in the PVR membrane of the TGFβ1-treated group, but only scanty αSMA positive myofibroblasts in the silibinin-treated group (Fig. 4F).

Silibinin Reduces the Phosphorylation and Nuclear Translocation of Smad3 and Suppresses Stat3 Phosphorylation

It is known that Smad-dependent pathway plays a central role in TGFβ-induced EMT of RPE cells. To investigate the underlying mechanism of silibinin-mediated inhibition of RPE EMT, we examined the effect of silibinin on TGFβ1-Smad signaling. To do this, we first treated ARPE-19 cells with 10 ng/mL TGFβ1 for distinct time points (0, 5, 15, 30, 60, and 120 minutes), and Western blot results showed that the phosphorylation of Smad3 started from 5 minutes and reached their peak at 60 minutes (Figs. 5A, 5B). We then selected 60 minutes to study the effect of silibinin on TGFβ1-Smad signaling. As Western blot results showed, silibinin treatment significantly inhibits the Smad3 phosphorylation in a dose-dependent manner (Figs. 5D, 5E). Notably, TGFβ1 treatment also induced the phosphorylation of Stat3 in ARPE-19 cells and silibinin treatment inhibited TGFβ1-induced Stat3 phosphorylation in a dose-dependent manner (see Figs. 5A, 5C, 5D, 5F). Moreover, immunofluorescence staining results showed silibinin treatment decreased the nuclear signals of Smad3 in ARPE-19 cells as compared to TGFβ1 treatment alone, indicating the inhibition effect of silibinin on TGFβ1-induced Smads nuclear translocation (Fig. 5G). Consistently, Western blot analysis showed silibinin treatment decreased the nuclear/cytoplasm ratio of Smad3 (Fig. 5H). In support of these findings, the bulk RNA-seq revealed that silibinin treatment globally reversed TGFβ1 Smad-dependent gene expression (Fig. 5I).

Discussion

The EMT of RPE cells is the key pathological process for PVR formation.[6] Retinal detachment due to the contraction of the transformed RPE cells within the proliferative membranes often results in significant vision loss.[2] Currently, it remains a lack of effective drugs to prevent PVR formation. In this study, we demonstrated that silibinin effectively inhibits TGFβ1-induced the EMT and cell migration of RPE cells in vitro. Silibinin also suppresses the formation of proliferative membranes in an intravitreal injected RPE-induced rat PVR model in vivo. Mechanistically, we found silibinin inhibits TGFβ1-induced Smad3 and Stat3 phosphorylation and Smad3 nuclear translocation. These findings suggest that silibinin may serve as a potential treatment for PVR.

Silymarin is a non-toxic polyphenolic flavonoid extracted from fruits and seeds of Silybum marianum, and silibinin is the main biologically active component in silymarin.[19] Silibinin possesses various biological properties, such as antifibrosis, anti-inflammatory, antioxidant, antiangiogenic, and pro-apoptotic capabilities.[10,20] Among these properties, its antifibrosis activities have been well studied. For instance, silibinin has been shown to inhibit liver fibrosis,[11] cigarette-induced pulmonary fibrosis,[21] and high-fat diet-induced renal fibrosis.[22] Importantly, silibinin has been clinically used to treat liver cirrhosis due to its strong antifibrosis effect.[11] Given that EMT is a key pathological process of fibrosis, the pronounced antifibrotic activity exhibited by silibinin implies its potential capability to inhibit EMT. In support of this notion, increasing evidence has demonstrated silibinin is able to suppress the EMT of various tumor cells, such as ovarian cancer, bladder cancer, prostate cancer, renal cell carcinoma, and non-small cell lung cancer.[13,15,23–26] Here, we demonstrated, for the first time, that silibinin inhibits EMT of RPE cells in vitro and PVR formation in an intravitreal injected RPE-induced rat PVR model.

RPE cell migration is a crucial step in the formation of proliferative membranes in PVR.[27,28] During the PVR formation, RPE cells first detach from Bruch's membrane and migrate to the epi-retinal or sub-retinal spaces where they interact with other cellular components and the extracellular matrix to form the proliferative membrane.[7,8] In our study, both scratch assay and transwell assay demonstrated that silibinin significantly inhibited the migration of RPE cells. PVR is considered a wound-healing response. During the healing process, the migrating cells produce various matrix metalloproteinases (MMPs) that degrade fibrin clots and replace them with extracellular matrix (ECM), such as collagen I to IV, fibronectin, laminin, proteoglycans, and hyaluronic acid.[29] This protease-mediated deposition and remodeling of the ECMs support and regulate cell migration.[30] Our study demonstrated that the levels of MMP2, fibronectin, and COL1A1, the α1 chain of collagen I, were significantly increased in the EMT process in RPE cells, and this elevation could be downregulated by silibinin. In support of these findings, our RNA-seq data revealed a global regulation of ECM formation- and remodeling-related genes by silibinin. In conclusion, silibinin-mediated inhibition of RPE cell migration may work through ECM regulation.

It is accepted that TGFβ is the strongest cytokine inducing the EMT of RPE cells during the PVR formation. Mechanistically, we demonstrated two possible mechanisms of silibinin-mediated inhibition of TGFβ-induced EMT of RPE cells: (1) by inhibiting Smad3 phosphorylation; and (2) by inhibiting Stat3 phosphorylation.

Upon the binding of TGFβ, the TGFβ type II receptor (TβRII) recruits and phosphorylates the TGFβ type I receptor (TβRI) which can further phosphorylate Smad2 and Smad3.[31] The phosphorylated Smad2 binds to phosphorylated Smad3 and further recruits Smad4 to form a heterotrimer. This heterotrimer subsequently translocates to the nucleus where they bind to the promoters of EMT-related genes to initiate their transcription.[32] In our study, we found silibinin inhibits Smad3 phosphorylation in a dose-dependent manner in the TGFβ1-induced EMT of RPE cells. In support of our findings, several studies have recently shown that silibinin can inhibit TGFβ1-induced Smads phosphorylation in other cell types for different biological events.

Investigative Ophthalmology & Visual Science

For instance, Verdura et al. demonstrated silibinin inhibits EMT of H2228/CR tumor cells through the suppression of TGFβ-induced SMAD2/3 phosphorylation.[33] Cho et al. reported silibinin suppresses TGFβ1-induced Smad2/3 phosphorylation to reduce type I collagen production in human skin fibroblasts.[34] Mechanistically, Chen et al. illustrated the inhibition of TGFβ1-induced Smads phosphorylation by silibinin is likely through the blockage of TβRII phosphorylation.[35] Whether silibinin-mediated inhibition of Smad3 phosphorylation in TGFβ1-induced EMT of RPE cells is through this mechanism or not remains to be defined.

In addition to the activation of the Smad-dependent pathway, we also observed the activation of Stat3 pathway, evidenced by Stat3 phosphorylation, upon the treatment of TGFβ1 in ARPE-19 cells. In support of this finding, several studies have demonstrated that independent of the Smad pathway, TGFβ1 can induce Stat3 phosphorylation likely through the activation of JAK1, an upstream kinase of Stat3 in other cell types.[36,37] More specifically, after TGFβ1 treatment, phosphorylated TβRI directly binds to and activates JAK1. Activated JAK1 can further phosphorylate Stat3.[37,38] Further evidence showed TGFβ-Jak1-Stat3 pathway is required to cooperate with Smad3 for mediating TGFβ-induced fibrotic response in hepatic stellate cells.[38] Mechanistically, phosphorylated Stat3 forms a complex with Smad3 and promotes its nuclear localization thereby enhancing fibrotic-related gene transcription.[38,39] In our study, we found that silibinin inhibited the Stat3 phosphorylation and the nuclear translocation of Smad3 protein in ARPE-19 cells, suggesting silibinin can not only directly inhibit the TGFβ-Smads pathway but also indirectly inhibit this pathway through the suppression of Stat3 phosphorylation (Fig. 5J).

Overall, our data demonstrated, we believe for the first time, that silibinin could inhibit the EMT of ARPE-19 cells in vitro and prevent PVR formation in vivo. Our study highlights a new perspective on the clinical treatment of PVR and provides a theoretical basis for the clinical application of silibinin for PVR.

Acknowledgments

Supported by China Postdoctoral Science Foundation (Project number 2022M713603), Guangdong Basic and Applied Basic Research Foundation (Project number 2021A1515111082), the Natural Science Foundation of Guangdong Province of China (Project numbers 2023A1515010159 and 2021A1515010513), and the National Natural Science Foundation of China (82171404).

Disclosure: **X. Ma**, None; **Y. Xie,** None; **Y. Gong**, None; **C. Hu**, None; **K. Qiu**, None; **Y. Yang**, None; **H. Shen**, None; **X. Zhou**, None; **C. Long**, None; **X. Lin**, None

References

1. Chiquet C, Rouberol F. [Proliferative vitreoretinopathy: prophylactic treatment]. *J Fr Ophtalmol*. 2014;37:737–743.
2. Claes C, Lafetá AP. Proliferative vitreoretinopathy. *Dev Ophthalmol*. 2014;54:188–195.
3. Idrees S, Sridhar J, Kuriyan AE. Proliferative vitreoretinopathy: a review. *Int Ophthalmol Clin*. 2019;59:221–240.
4. Hirose F, Kiryu J, Tabata Y, et al. Experimental proliferative vitreoretinopathy in rabbits by delivery of bioactive proteins with gelatin microspheres. *Eur J Pharm Biopharm*. 2018;129:267–272.
5. Ishikawa K, He S, Terasaki H, et al. Resveratrol inhibits epithelial-mesenchymal transition of retinal pigment epithelium and development of proliferative vitreoretinopathy. *Sci Rep*. 2015;5:16386.
6. Yang S, Li H, Li M, Wang F. Mechanisms of epithelial-mesenchymal transition in proliferative vitreoretinopathy. *Discov Med*. 2015;20:207–217.
7. Zou H, Geathers JS, Grillo SL, et al. Polarity and epithelial-mesenchymal transition of retinal pigment epithelial cells in proliferative vitreoretinopathy. *PeerJ*. 2020;8:e10136.
8. Feist RM, King JL, Morris R, Witherspoon CD, Guidry C. Myofibroblast and extracellular matrix origins in proliferative vitreoretinopathy. *Graefes Arch Clin Exp Ophthalmol*. 2014;252:347–357.
9. Shukal D, Bhadresha K, Shastri B, Mehta D, Vasavada A, Johar K. Dichloroacetate prevents TGFbeta-induced epithelial-mesenchymal transition of retinal pigment epithelial cells. *Exp Eye Res*. 2020;197:108072.
10. Singh M, Kadhim MM, Turki Jalil A, et al. A systematic review of the protective effects of silymarin/silibinin against doxorubicin-induced cardiotoxicity. *Cancer Cell Int*. 2023;23:88.
11. Abenavoli L, Capasso R, Milic N, Capasso F. Milk thistle in liver diseases: past, present, future. *Phytother Res*. 2010;24:1423–1432.
12. Ferenci P, Scherzer TM, Kerschner H, et al. Silibinin is a potent antiviral agent in patients with chronic hepatitis C not responding to pegylated interferon/ribavirin therapy. *Gastroenterology*. 2008;135:1561–1567.
13. Li F, Sun Y, Jian J, et al. Silibinin attenuates TGF–β1–induced migration and invasion via EMT suppression and is associated with COX–2 downregulation in bladder transitional cell carcinoma. *Oncol Rep*. 2018;40:3543–3550.
14. Nambiar DK, Rajamani P, Singh RP. Silibinin attenuates ionizing radiation-induced pro-angiogenic response and EMT in prostate cancer cells. *Biochem Biophys Res Commun*. 2015;456:262–268.
15. Fan Y, Hou T, Dan W, et al. Silibinin inhibits epithelial–mesenchymal transition of renal cell carcinoma through autophagy–dependent Wnt/β–catenin signaling. *Int J Mol Med*. 2020;45:1341–1350.
16. Ma X, Long C, Wang F, et al. METTL3 attenuates proliferative vitreoretinopathy and epithelial-mesenchymal transition of retinal pigment epithelial cells via wnt/beta-catenin pathway. *J Cell Mol Med*. 2021;25:4220–4234.
17. He J, Long C, Huang Z, et al. PTEN reduced UVB-mediated apoptosis in retinal pigment epithelium cells. *Biomed Res Int*. 2017;2017:3681707.
18. Behar-Cohen FF, Thillaye-Goldenberg B, de Bizemont T, Savoldelli M, Chauvaud D, de Kozak Y. EIU in the rat promotes the potential of syngeneic retinal cells injected into the vitreous cavity to induce PVR. *Invest Ophthalmol Vis Sci*. 2000;41:3915–3924.
19. Abenavoli L, Izzo AA, Milić N, Cicala C, Santini A, Capasso R. Milk thistle (Silybum marianum): a concise overview on its chemistry, pharmacological, and nutraceutical uses in liver diseases. *Phytother Res*. 2018;32:2202–2213.
20. Sahu R, Goswami S, Narahari Sastry G, Rawal RK. The preventive and therapeutic potential of the flavonoids in liver cirrhosis: current and future perspectives. *Chem Biodivers*. 2023;20:e202201029.
21. Ko JW, Shin NR, Park SH, et al. Silibinin inhibits the fibrotic responses induced by cigarette smoke via suppression of TGF-beta1/Smad 2/3 signaling. *Food Chem Toxicol*. 2017;106:424–429.
22. Liu K, Zhou S, Liu J, Wang Y, Zhu F, Liu M. Silibinin attenuates high-fat diet-induced renal fibrosis of diabetic nephropathy. *Drug Des Devel Ther*. 2019;13:3117–3126.

23. Sun Y, Guan Z, Zhao W, et al. Silibinin suppresses bladder cancer cell malignancy and chemoresistance in an NF-kappaB signal-dependent and signal-independent manner. *Int J Oncol*. 2017;51:1219–1226.
24. Maleki N, Yavari N, Ebrahimi M, et al. Silibinin exerts anticancer activity on human ovarian cancer cells by increasing apoptosis and inhibiting epithelial-mesenchymal transition (EMT). *Gene*. 2022;823:146275.
25. Wu KJ, Zeng J, Zhu GD, et al. Silibinin inhibits prostate cancer invasion, motility and migration by suppressing vimentin and MMP-2 expression. *Acta Pharmacol Sin*. 2009;30:1162–1168.
26. Xu S, Zhang H, Wang A, Ma Y, Gan Y, Li G. Silibinin suppresses epithelial-mesenchymal transition in human non-small cell lung cancer cells by restraining RHBDD1. *Cell Mol Biol Lett*. 2020;25:36.
27. Datlibagi A, Zein-El-Din A, Frohly M, Willermain F, Delporte C, Motulsky E. Experimental models to study epithelial-mesenchymal transition in proliferative vitreoretinopathy. *Int J Mol Sci*. 2023;24:4509.
28. Ouyang S, Ji D, He S, Xia X. Endoplasmic reticulum stress as a novel target to inhibit transdifferentiation of human retinal pigment epithelial cells. *Front Biosci (Landmark Ed)*. 2022;27:38.
29. Bainbridge P. Wound healing and the role of fibroblasts. *J Wound Care*. 2013;22:407–408, 410–412.
30. Rauch U, Schafer KH. The extracellular matrix and its role in cell migration and development of the enteric nervous system. *Eur J Pediatr Surg*. 2003;13:158–162.
31. Wrighton KH, Lin X, Feng XH. Phospho-control of TGF-beta superfamily signaling. *Cell Res*. 2009;19:8–20.
32. Schiller M, Javelaud D, Mauviel A. TGF-beta-induced SMAD signaling and gene regulation: consequences for extracellular matrix remodeling and wound healing. *J Dermatol Sci*. 2004;35:83–92.
33. Verdura S, Encinar JA, Teixidor E, et al. Silibinin overcomes EMT-driven lung cancer resistance to new-generation ALK inhibitors. *Cancers (Basel)*. 2022;14:6101.
34. Cho JW, Il KJ, Lee KS. Downregulation of type I collagen expression in silibinin-treated human skin fibroblasts by blocking the activation of Smad2/3-dependent signaling pathways: potential therapeutic use in the chemoprevention of keloids. *Int J Mol Med*. 2013;31:1148–1152.
35. Chen YH, Liang CM, Chen CL, et al. Silibinin inhibits myofibroblast transdifferentiation in human tenon fibroblasts and reduces fibrosis in a rabbit trabeculectomy model. *Acta Ophthalmol*. 2013;91:e506–515.
36. Guadagnin E, Narola J, Bonnemann CG, Chen YW. Tyrosine 705 phosphorylation of STAT3 is associated with phenotype severity in TGFbeta1 transgenic mice. *Biomed Res Int*. 2015;2015:843743.
37. Wang F, Wang S, Zhang C, et al. Noncanonical JAK1/STAT3 interactions with TGF-beta modulate myofibroblast transdifferentiation and fibrosis. *Am J Physiol Lung Cell Mol Physiol*. 2022;323:L698–L714.
38. Tang LY, Heller M, Meng Z, et al. Transforming growth factor-beta (TGF-beta) directly activates the JAK1-STAT3 axis to induce hepatic fibrosis in coordination with the SMAD pathway. *J Biol Chem*. 2017;292:4302–4312.
39. Itoh Y, Saitoh M, Miyazawa K. Smad3-STAT3 crosstalk in pathophysiological contexts. *Acta Biochim Biophys Sin (Shanghai)*. 2018;50:82–90.

Investigative Ophthalmology & Visual Science